

# Isostructural diamagnetic cobalt(III) and paramagnetic nickel(III) dithiolene complexes with an extended benzenedithiolate core [CpM<sup>III</sup>(bdtodt)] (M = Co and Ni)

Mitsushiro Nomura, Marc Fourmigué \*

Sciences Chimiques de Rennes, UMR 6226 CNRS-Université de Rennes 1, Equipe MaCSE, Campus de Beaulieu, 35042 Rennes cedex, France

Received 16 November 2006; received in revised form 19 February 2007; accepted 20 February 2007

Available online 25 February 2007

## Abstract

The isostructural diamagnetic [CpCo(bdtodt)] and paramagnetic [CpNi(bdtodt)] (Cp =  $\eta^5$ -cyclopentadienyl, bdtodt:benzo[1,3]dithiol-2-one-5,6-dithiolato) complexes were prepared by starting from the corresponding bis(dithiocarbonate): benzo[1,2-d;4,5-d']bis[1,3]dithiole-2,6-dione. Both Co and Ni complexes are isostructural and crystallize in the orthorhombic system, space group *Pbca*. The formally M<sup>III</sup> (16-electron for Co<sup>III</sup> and 17-electron Ni<sup>III</sup>) complexes were investigated by X-ray structure analyses and exhibit the same two-legged piano-stool geometry. The CV of the radical [CpNi(bdtodt)] resulted in well-defined reversible reduction and oxidation waves. On the other hand, oxidation of [CpCo(bdtodt)] leads to dimerization in CH<sub>2</sub>Cl<sub>2</sub> or reaction in the more coordinating CH<sub>3</sub>CN solvent. The absorption maximum ( $\lambda_{\text{max}}$ ) of [CpNi(bdtodt)] (741 nm) showed a more red shift compared with [CpCo(bdtodt)] (595 nm) in dichloromethane solution. The structural similarities, and electrochemical, spectroscopic and magnetic differences between various [CpCo(dithiolene)] and [CpNi(dithiolene)] complexes are further analyzed.

© 2007 Elsevier B.V. All rights reserved.

**Keywords:** Dithiolene; Nickel; Cobalt; Electrochemistry; Crystal structures

## 1. Introduction

Homoleptic metal dithiolene complexes [1], which involve bis(dithiolene) [M(dithiolene)<sub>2</sub>]<sup>n-</sup> (M = Ni, Pd, Pt) [2], tris(dithiolene) [M(dithiolene)<sub>3</sub>]<sup>n-</sup> (M = V, Cr, Mo, W, Re [3], Nd, Ce [4], U [5]) and tetrakis(dithiolene) [M(dithiolene)<sub>4</sub>]<sup>n-</sup> (M = U) [5], are composed of only dithiolene ligands. Heteroleptic dithiolene complexes, which involve dithiolene ligand and other ligands, are also known with various co-ligands [6]. Among them, sandwich or half-sandwich metal dithiolene complexes [Cp<sub>n</sub>M(dithiolene)<sub>n</sub>] can be classified into four main categories, according to the ratio of Cp and dithiolene ligands: [Cp<sub>2</sub>M(dithiolene)] (Cp/dithiolene ratio = 2:1 complex), [CpM(dithiolene)<sub>2</sub>] (1:2 complex),

[CpM(dithiolene)<sub>2</sub>] (bimetallic 1:1 complex), and [CpM(dithiolene)] (1:1 complex) [7].

Among them, different series of *paramagnetic* complexes [8] such as the d<sup>1</sup> [Cp<sub>2</sub>Mo(dithiolene)]<sup>+</sup> were also described, showing a wide variety of magnetic behaviors, from uniform spin chains to spin ladders or antiferromagnetic ground states [9]. In addition, the paramagnetic, formally d<sup>7</sup>, [CpNi(dithiolene)] complexes are also very interesting species, as they are neutral organometallic radicals (*S* = 1/2) [10]. These new series of organometallic neutral radical complexes exhibit antiferromagnetic interactions in the solid state, not only through dithiolene/dithiolene intermolecular interactions as usually observed among these complexes but also through a striking Cp···Cp face-to-face overlap [10c]. We have recently developed the preparation methods, physical properties, and crystal structures of [CpNi(S<sub>2</sub>C<sub>2</sub>R<sub>2</sub>)] [10b], [CpNi(dmit)] [10a], [CpNi(dddt)], [CpNi(bdt)] [10c], and [CpNi(pdtd)] [10d]

\* Corresponding author. Tel.: +33 2 23 23 52 43; fax: +33 2 23 23 67 32.  
E-mail address: [marc.fourmigue@univ-rennes1.fr](mailto:marc.fourmigue@univ-rennes1.fr) (M. Fourmigué).

series including analogous [CpNi(diselenolene)] complexes (Chart 1).

Note that the S/Se exchange in the metallacycle does not modify the crystal packing in [CpNi(dichalcogenolene)] complexes. Isostructural pairs are indeed observed in [CpNi(dddt)] *vs.* [CpNi(ddds)] [10c] (monoclinic,  $P2_1$ ), [CpNi(dmit)] *vs.* [CpNi(dsit)] [10a] (monoclinic,  $P2_1$ ), and [CpNi(bdt)] *vs.* [CpNi(bds)] [10c] (monoclinic,  $P2_1/c$ ). Probably, the Cp ring partially hides the  $MS_2$  and  $MSe_2$  moiety engaged in the metal coordination. On the other hand, even “slight” modifications of the outer substituents of the dithiolene or diselenolene core can modify strongly the crystal packing. For example, [CpNi(dsdt)] [10c] (monoclinic,  $P2_1/n$ ) is not isostructural with [CpNi(dddt)] or [CpNi(ddds)].

We wanted to investigate if this isostructural character upon S/Se exchange in the nickel series was also maintained upon *metal* substitution and decide to compare the [CpNi<sup>III</sup>(dithiolene)] complexes with the corresponding cobalt [CpCo<sup>III</sup>(dithiolene)] complexes, which exhibit different electron counts (16- or 17-electron for the Co and Ni, respectively) on the metal centers. The isostructural character is indeed prerequisite if one wants to investigate the single crystal EPR properties of a paramagnetic nickel [CpNi(dithiolene)] complex, when diluted in the corresponding diamagnetic cobalt [CpCo(dithiolene)] crystalline matrix. In fact, only two isostructural pairs are known, in [CpCo(mnt)] [11] *vs.* [CpNi(mnt)] [10b] (monoclinic,  $C2/c$  space group), and [CpCo(bdt)] (monomer) [12a] *vs.* [CpNi(bdt)] [10c] (monoclinic,  $P2_1/c$ ), while, [CpCo(dmit)] (monoclinic,  $P2_1/n$ ) [12b] and [CpNi(dmit)] (monoclinic,  $P2_1$ ) [10a], albeit not isostructural, are closely related and differ by a disorder affecting the Cp ring in [CpNi(dmit)].

We report here on two isostructural [CpCo(dithiolene)] and [CpNi(dithiolene)] complexes based on the benzo[1,3]-dithiol-2-one-5,6-dithiolate (bdtodt) ligand to give the mononuclear [CpCo(bdtodt)] and [CpNi(bdtodt)] complexes. Their syntheses, structures, electrochemical behavior and electronic absorption are investigated. We discuss here on the structural similarity, and also the electrochemical, spectroscopic and magnetic differences between various [CpCo(dithiolene)] and [CpNi(dithiolene)] complexes.

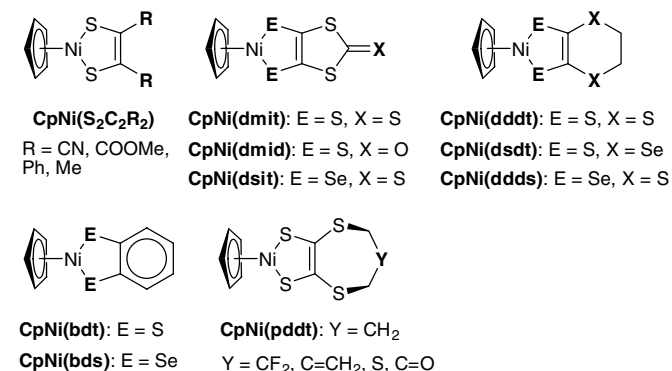


Chart 1.

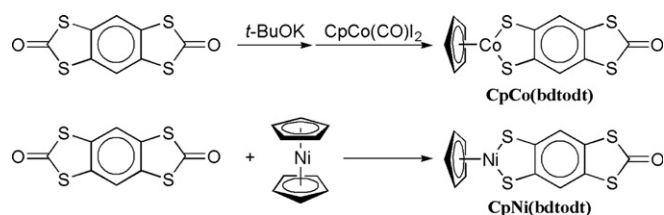
## 2. Results and discussion

### 2.1. Preparations of [CpCo(bdtodt)] and [CpNi(bdtodt)] complexes

During our attempts to prepare bimetallic derivatives of the benzene tetrathiolate (btt) tetra anion from the reaction of the bis(dithiocarbonate) benzo[1,2-d;4,5-d']bis[1,3]dithiole-2,6-dione with different Ni or Co metal sources, we have observed the preferential formation of the monometallic derivatives, incorporating the bdtodt (bdtodt: benzo[1,3]dithiol-2-one-5,6-dithiolato) dithiolate ligand. For example, the preparations of [CpCo(dithiolene)] complexes are well known [8,13,14] and involve the reaction of [CpCo(CO)I<sub>2</sub>] with 1,2-dithiolate dianion. Accordingly, the bis(dithiocarbonate) benzo[1,2-d;4,5-d']bis[1,3]dithiole-2,6-dione was reacted with potassium *tert*-butoxide (4 equiv.) in THF for 30 min (Scheme 1). After [CpCo(CO)I<sub>2</sub>] was added into the reaction mixture, the solution color was changed from yellow to dark blue. A blue fraction was separated by column chromatography on silica gel. The monometallic dark blue solid [CpCo(bdtodt)] was obtained in 55% yield but no bimetallic derivative could be isolated.

Convenient methods for [CpNi(dithiolene)] complexes have been not developed until recently. King first reported in 1963, the synthesis of [CpNi(tfd)] (tfd = bis(trifluoromethyl)-1,2-dithiolate) by the reaction of [CpNi(CO)]<sub>2</sub> with bis(trifluoromethyl)dithiete (S<sub>2</sub>C<sub>2</sub>(CF<sub>3</sub>)<sub>2</sub>) [15]. Faulmann et al. serendipitously observed the interesting reaction of [Cp<sub>2</sub>Ni](BF<sub>4</sub>) with Na[Ni(dmit)<sub>2</sub>] to form [CpNi(dmit)] [16]. After that, we have recently reported improved methods for the preparation of the [CpNi(S<sub>2</sub>C<sub>2</sub>R<sub>2</sub>)], [CpNi(dddt)], [CpNi(bdt)] and [CpNi(pddt)] series (Chart 1) [10]. In this work, we choose the thermal activation of 1,3-dithiol-2-one moiety which can produce better yield than 1,2-dithiolate to form [CpNi(dithiolene)] complexes [10c]. This activation reaction of 1,3-dithiol-2-one derivative has been reported to generate the oxidized species of 1,2-dithiolate (neutral 1,2-dithioketone or 1,2-dithiete) as a reaction intermediate [17]. Thus, nickelocene ([Cp<sub>2</sub>Ni]) directly reacted with benzo[1,2-d;4,5-d']bis[1,3]dithiole-2,6-dione in refluxing toluene for 24 h to give the dark red solid [CpNi(bdtodt)] in 26% yield (Scheme 1).

Note that other dithiolene complexes with this bdtodt dithiolate ligand have already been reported, as the square-planar Ni and Au complexes [M(bdtodt)<sub>2</sub>]<sup>−</sup>



Scheme 1.

[18,19] and the titanocene complex [Cp<sub>2</sub>Ti(bdtodt)] [20]. The possible dinuclear complexes such as [CpM(btt)MCp] were not obtained in the reaction shown in Scheme 1. The reason may be the very poor solubility of the dinuclear complexes. The η<sup>5</sup>-pentamethylcyclopentadienyl (Cp\*) can be introduced instead of Cp ligand for increasing their solubility. This investigation is now in progress. Some examples of dinuclear complexes with (btt) cores have been reported in the [(triphos)Co(btt)Co(triphos)] [21] and [Cp<sub>2</sub>M(btt)MCp<sub>2</sub>] (M = Ti, Zr and Hf) complexes [22].

## 2.2. X-ray crystal structures of [CpCo(bdtodt)] and [CpNi(bdtodt)] complexes

The molecular structures of [CpCo(bdtodt)] and [CpNi(bdtodt)] were determined by X-ray structure analyses. The ORTEP drawings are shown in Fig. 1, and their selected bond lengths and angles are summarized in Table 1 which also includes the bond lengths and angles of [CpCo(bdt)] (bdt = 1,2-benzenedithiolate) and [CpNi(bdt)] for comparison.

[CpCo(bdtodt)] and [CpNi(bdtodt)] are isostructural and crystallize in the orthorhombic system, space groups *Pbca*. Such crystallographic similarity has already been observed between some [CpCo(dithiolene)] and [CpNi(dithiolene)] complexes [10–12]. Fig. 1 shows typical two-legged piano-stool geometries composed from Cp and bidentate dithiolene ligands with planarity of Cp ligand, metallacycle (MS<sub>2</sub>C<sub>2</sub> moiety) and benzene ring. The Ni–S bond length in [CpNi(bdtodt)] is slightly longer than the Co–S in [CpCo(bdtodt)]. This tendency has been also observed in [CpCo(bdt)] *vs.* [CpNi(bdt)] [10c] (in Table 1), also [CpCo(mnt)] (2.110 Å) [11] *vs.* [CpNi(mnt)] (2.1255 Å) [10b], and [CpCo(dmit)] (2.1233 Å) [12b] *vs.* [CpNi(dmit)] (2.138 Å) [10a]. In general, the strong π-donation from sulfur to metal center in the metalladithiolene ring can shorten the M–S bond length [23]. This result

explains that such π-donation in the 16-electron [CpCo(dithiolene)] complex is stronger than that in the 17-electron [CpNi(dithiolene)] complex.

It is known that the 16 e complexes such as [CpCo(bdt)] can form a dimer in the solid state through Co⋯S intermolecular interactions. In [CpCo(bdt)], the dimer can be changed to the corresponding monomer in the single crystal upon warming above 150 °C [12a]. Note here that [CpCo(bdtodt)] crystallized as a monomer at room temperature.

## 2.3. Electrochemistry of [CpCo(bdtodt)] and [CpNi(bdtodt)] complexes

The cyclic voltammograms (CV) of [CpCo(bdtodt)] and [CpNi(bdtodt)] are shown in Fig. 2, and their redox potentials are displayed in Table 2. The CV of [CpNi(bdtodt)] resulted in two well-defined reversible reduction and oxidation waves at –0.83 V and +0.38 V (*vs.* Fc/Fc<sup>+</sup>), respectively (Fig. 2a). On the other hand, the CV of [CpCo(bdtodt)] exhibited a reversible reduction wave at –0.97 V in CH<sub>2</sub>Cl<sub>2</sub> or at –0.91 V in CH<sub>2</sub>Cl<sub>2</sub>/MeCN (1:1 mixture). An irreversible oxidation wave is observed at +0.62 V in CH<sub>2</sub>Cl<sub>2</sub> (Fig. 2b), which becomes an irreversible oxidation process with two steps at +0.38 V and +0.84 V if the electrochemical investigation is performed in CH<sub>2</sub>Cl<sub>2</sub>/MeCN (Fig. 2c).

The first redox potentials of [CpCo(bdtodt)] and [CpNi(bdtodt)] are more positive than those of the [CpCo(bdt)] and [CpNi(bdt)], respectively (Table 2). This result suggests an electron-withdrawing effect of the dithiocarbonate group. The difference between oxidation and reduction potential ( $\Delta E_{1/2} = |E_{1/2}(\text{ox}) - E_{1/2}(\text{red})|$ ) of [CpNi(dithiolene)] complex is smaller than the  $\Delta E_{1/2}$  value of [CpCo(dithiolene)] complex (Table 2). This result correlates with a red shift of absorption maximum in [CpNi(dithiolene)] complex (see Table 3 and Section 2.4).

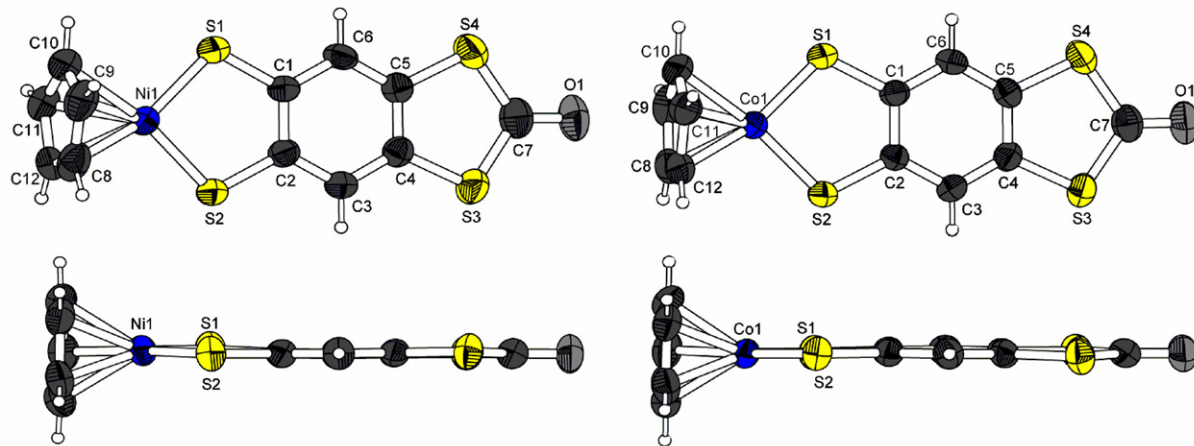


Fig. 1. The ORTEP drawings of isostructural [CpNi(bdtodt)] and [CpCo(bdtodt)]: (top left) [CpNi(bdtodt)] showing the all atoms, (bottom left) side view of [CpNi(bdtodt)] from dithiolene and benzene planes, (top right and bottom right) [CpCo(bdtodt)]. The thermal ellipsoids are drawn at 50% probability level.

Table 1  
Selected bond lengths and angles

	[CpCo(bdtodt)]	[CpCo(bdt)] (monomer) <sup>b</sup>	[CpNi(bdtodt)]	[CpNi(bdt)] <sup>c</sup>
<i>Bond length</i>				
M1–S1	2.1113(10)	2.111(2)	2.1272(16)	2.1205(13)
M1–S2	2.1201(10)	2.111(2)	2.1395(16)	2.1280(13)
S1–C1	1.732(3)	1.729(7)	1.739(6)	1.731(5)
S2–C2	1.727(3)	1.748(6)	1.741(5)	1.740(4)
C1–C2	1.414(4)	— <sup>a</sup>	1.407(7)	1.410(6)
C2–C3	1.405(5)	— <sup>a</sup>	1.399(8)	1.395(6)
C3–C4	1.378(5)	— <sup>a</sup>	1.403(8)	1.371(7)
C4–C5	1.410(5)	— <sup>a</sup>	1.394(8)	1.384(8)
C5–C6	1.372(5)	— <sup>a</sup>	1.382(8)	1.373(8)
C6–C1	1.394(5)	— <sup>a</sup>	1.403(7)	1.399(6)
<i>Bond angles</i>				
S1–M1–S2	92.53(4)	91.9(1)	93.74(6)	93.93(5)
M1–S1–C1	105.49(11)	105.9(2)	103.73(18)	103.71(15)
M1–S2–C2	105.25(12)	106.1(2)	103.8(2)	103.61(15)
S1–C1–C2	118.2(3)	118.9(5)	119.8(4)	119.6(3)
S2–C2–C1	118.5(3)	117.2(5)	118.9(4)	118.8(3)

<sup>a</sup> Not available.

<sup>b</sup> Ref. [12a].

<sup>c</sup> Ref. [10c].

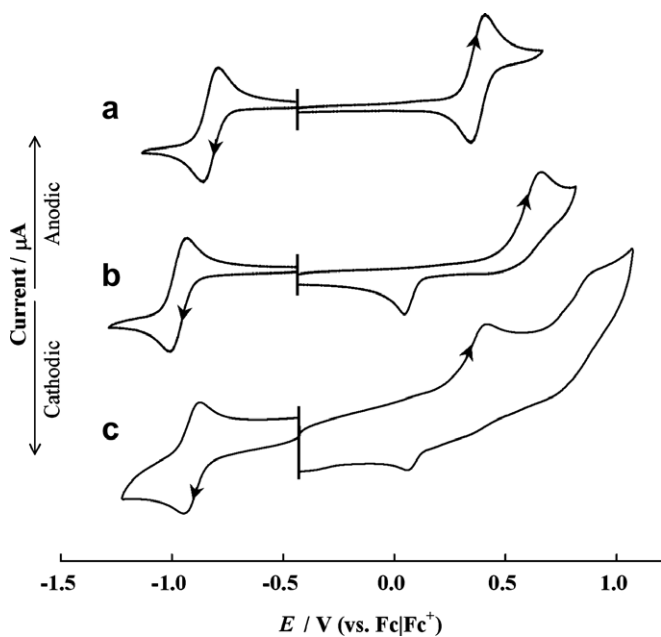


Fig. 2. Cyclic voltammograms of: (a) [CpNi(bdtodt)] in CH<sub>2</sub>Cl<sub>2</sub>, (b) [CpCo(bdtodt)] in CH<sub>2</sub>Cl<sub>2</sub> and (c) [CpCo(bdtodt)] in CH<sub>2</sub>Cl<sub>2</sub> + MeCN (1:1(v/v)). Scan rate = 100 mV s<sup>-1</sup>, Pt disk as a working electrode (1.0 mm in diameter), supporting electrolyte *n*-Bu<sub>4</sub>NPF<sub>6</sub> (0.1 M).

The irreversible oxidation wave of [CpCo(bdtodt)] indicates that its oxidized species is not stable on the time scale of CV ( $v = 100$  mV/s). In general, the [CpCo<sup>III</sup>(dithiolene)] complexes are electron-deficient because of a formal 16-electron complex. Namely, they are not stable for a chemical or an electrochemical oxidation. The oxidized species of [CpCo(dithiolene)] undergoes a dimerization or a solvent coordination to the metal center. Indeed, [Cp<sup>\*</sup>Co(ddd)] and [Cp<sup>\*</sup>Co( $\mu$ -C<sub>2</sub>S<sub>4</sub>)CoCp<sup>\*</sup>] have been reported to

dimerize in CH<sub>2</sub>Cl<sub>2</sub> or to react with MeCN after an electrochemical oxidation (EC reaction) [25,26]. In addition, the isoelectronic [( $\eta^6$ -arene)Ru<sup>II</sup>(dithiolene)] complexes can also dimerize by an electrochemical oxidation [27]. In our case, [CpCo(bdtodt)] probably forms a dimer upon electrochemical oxidation in CH<sub>2</sub>Cl<sub>2</sub> solution (Scheme 2). Furthermore, the same CVs were repeated through multiple scan processes (not shown). This result indicates that the dimer generated on the electrode is reduced around +0.1 V (Fig. 2b) to regenerate the original monomer complex. The electrochemical square scheme [28] shown in Scheme 2, describes this monomer–dimer structure changes (ECEC reaction).

In addition, if one introduces a coordinating solvent as CH<sub>3</sub>CN, the oxidation potential is moved toward cathodic potentials by 230 mV while the reduction potential is only slightly modified. A similar behavior was already noticed in [Cp<sup>\*</sup>Co( $\mu$ -C<sub>2</sub>S<sub>4</sub>)CoCp<sup>\*</sup>] [26], and attributed to the influence of the kinetics of the acetonitrile coordination following the electron transfer (Scheme 1). Indeed, the similar reduction potential and spectroscopic properties in CH<sub>2</sub>Cl<sub>2</sub> and CH<sub>2</sub>Cl<sub>2</sub>/CH<sub>3</sub>CN indicate that the CH<sub>3</sub>CN coordination does not take place before oxidation. The second oxidation wave observed in CH<sub>2</sub>Cl<sub>2</sub>/MeCN, which was not found in pure CH<sub>2</sub>Cl<sub>2</sub>, is thus attributable to the formation of a dicationic MeCN adduct, [CpCo(bdtodt)(CH<sub>3</sub>CN)]<sup>2+</sup>.

#### 2.4. Electronic absorption spectra of [CpCo(bdtodt)] and [CpNi(bdtodt)] complexes

The electronic absorption maxima ( $\lambda_{\max}$ /nm) of [CpCo(dithiolene)] and [CpNi(dithiolene)] complexes are summarized in Table 3. The UV–Vis–NIR spectra (250–900 nm range) of [CpCo(bdtodt)] and [CpNi(bdtodt)] are shown in Fig. 3. Those complexes showed strong elec-

Table 2  
Redox potentials of [CpM(dithiolene)] (M = Co, Ni) complexes ( $E_{1/2}$  values vs.  $\text{Fc}^+/\text{Fc}$ )

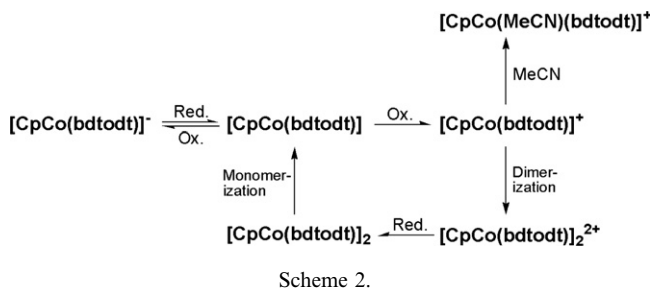
	Solv.	$E_{1/2}(\text{red})/\text{V}$	$\Delta E_p/\text{mV}$	$E_{1/2}(\text{ox})/\text{V}$	$\Delta E_p/\text{mV}$	Ref.
CpCo(dithiolene)						
[CpCo(bdt)]	MeCN	-1.00	57	+0.38	-	[11]
[CpCo(bdtodt)]	$\text{CH}_2\text{Cl}_2$	-0.97	64	+0.62 <sup>a</sup>	-	This work
[CpCo(bdtodt)]	$\text{CH}_2\text{Cl}_2 + \text{MeCN}$	-0.91	57	+0.39 <sup>a</sup>	-	This work
[CpCo(mnt)]	MeCN	-0.62	56	+0.71 <sup>b</sup>	79	[24]
CpNi(dithiolene)						
[CpNi(ddd)]	$\text{CH}_2\text{Cl}_2$	-1.06	106	-0.02	106	[10c]
[CpNi(bdt)]	$\text{CH}_2\text{Cl}_2$	-1.00	92	+0.30	88	[10c]
[CpNi(bdtodt)]	$\text{CH}_2\text{Cl}_2$	-0.83	63	+0.38	60	This work
[CpNi(dmit)]	$\text{CH}_2\text{Cl}_2$	-0.72	100	+0.28	100	[10c]
[CpNi(mnt)]	$\text{CH}_2\text{Cl}_2$	-0.64	-	+0.79 <sup>a</sup>	-	[10b]

<sup>a</sup> Irreversible.

<sup>b</sup> The oxidation potential of the corresponding MeCN adduct [CpCo(MeCN)(mnt)].

Table 3  
UV-Vis-NIR data ( $\lambda_{\text{max}}/\text{nm}$ ) of [CpCo(dithiolene)] and [CpNi(dithiolene)] complexes

Co dithiolene	$\lambda_{\text{max}}/\text{nm}$	Solv.	Ref.	Ni dithiolene	$\lambda_{\text{max}}/\text{nm}$	Solv.	Ref.
[CpCo( $\text{S}_2\text{C}_2(\text{CO}_2\text{Me})_2$ )]	550	MeCN	[30]	[CpNi( $\text{S}_2\text{C}_2(\text{CO}_2\text{Me})_2$ )]	695	$\text{CH}_2\text{Cl}_2$	[10b]
[CpCo(mnt)]	572	$\text{CH}_2\text{Cl}_2$	[29]	[CpNi(mnt)]	698	$\text{CH}_2\text{Cl}_2$	[10b]
[CpCo(bdt)]	566	MeCN	[30]	[CpNi(bdt)]	722	$\text{CH}_2\text{Cl}_2$	[10c]
[CpCo(bdtodt)]	595	$\text{CH}_2\text{Cl}_2$	This work	[CpNi(bdtodt)]	741	$\text{CH}_2\text{Cl}_2$	This work
[CpCo( $\text{S}_2\text{C}_2\text{Ph}_2$ )]	600	MeCN	[30]	[CpNi( $\text{S}_2\text{C}_2\text{Ph}_2$ )]	846	$\text{CH}_2\text{Cl}_2$	[10b]
[CpCo(dmit)]	678	$\text{CH}_2\text{Cl}_2$	This work	[CpNi(dmit)]	967	$\text{CH}_2\text{Cl}_2$	[10c]
				[CpNi(ddd)]	1012	$\text{CH}_2\text{Cl}_2$	[10c]



tronic absorptions at 595 nm for [CpCo(bdtodt)] and 741 nm for [CpNi(bdtodt)], respectively.

According to Table 3, the  $\lambda_{\text{max}}$  of [CpNi(dithiolene)] complexes always show a larger red shift than the corresponding [CpCo(dithiolene)] complexes, amounting to 120–290 nm. Note that the electron-rich (or sulfur-rich) complexes such as [CpNi(ddd)] and [CpNi(dmit)] exhibit a remarkable red shift. This tendency is supported by the CV data ( $\Delta E_{1/2}$ ) in Table 2. In this work, we found that [CpNi(dithiolene)] complexes usually show their absorption maxima in NIR region, except for electron-poor complexes ([CpNi(mnt)] [29] and [CpNi( $\text{S}_2\text{C}_2(\text{CO}_2\text{Me})_2$ )] [30]) or in the benzenedithiolate series [10c], as indeed observed here for [CpNi(bdtodt)].

### 2.5. Solid state properties

As both compounds are isostructural, we will limit here the description to the paramagnetic [CpNi(bdtodt)] com-

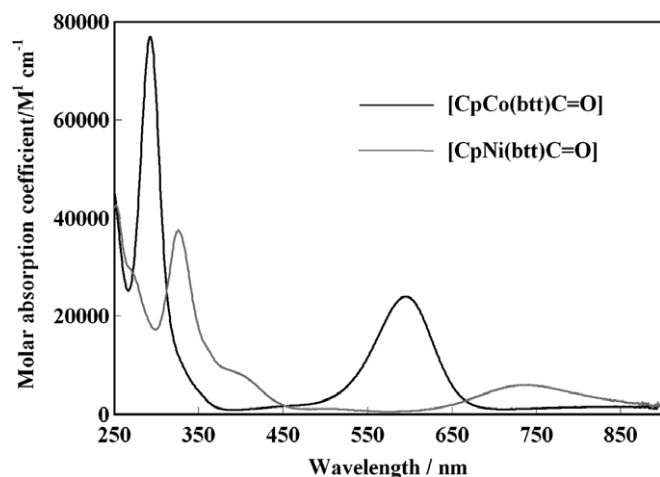


Fig. 3. UV-Vis-NIR spectra of [CpCo(bdtodt)] (black line) and [CpNi(bdtodt)] (gray line) in dichloromethane solution.

plex, in order to correlate its structural organization to its magnetic behavior. In the solid state, molecules of [CpNi(bdtodt)] complexes are associated into layers (Fig. 4) through a short  $\text{C-H}\cdots\text{O}=\text{C}$  hydrogen bond with following structural features:  $(\text{C}-)\text{H}\cdots\text{O}$ : 2.48 Å,  $\text{C}(\text{-H})\cdots\text{O}$ : 3.376(9) and  $\text{C}-\text{H}\cdots\text{O}$ : 161.8°. Such weak  $\text{C}-\text{H}\cdots\text{X}$  hydrogen bonds are now recognized to have an important structural role in influencing, moderating or complementing stronger forces, to the point where they have been shown in several instances to direct the

formation of specific structural patterns [31]. Their influence in the molecular packing of *paramagnetic* species in conducting or magnetic systems has also been noted in many examples [9a,32]. These hydrogen bonded planes pile up on top of each other along the *a* axis as shown in Fig. 5, leading to the formation of slabs perpendicular to *c*, connected to each other by the hydrogen bond network.

Within these layers, molecules are associated into inversion-centered dyads, connected to each other along the *b* direction through S··S intermolecular interactions (Fig. 6). The shortest intermolecular S··S contacts are found at 3.636(2) Å and involve one sulfur atom of the metallacycle and one sulfur atom of the outer dithiole-2-one ring. Intermolecular distances within the inversion-centered dyad are much longer, at 3.929 and 4.098 Å. This structural characteristics, combined with the fact that the spin density in this class of complexes is essentially concentrated on the metallacycle [10c] let us anticipate that the intermolecular magnetic interactions between the radical species will be weak, as indeed deduced from the temperature dependence of the magnetic susceptibility of [CpNi(bdtodt)] (Fig. 7). It follows a Curie–Weiss behavior at high temperatures with a Curie–Weiss temperature of 21 K, demonstrating the presence of antiferromagnetic interactions. The presence of a rounded susceptibility maximum at  $T_{\chi_{\max}} = 22$  K is indicative of a Heisenberg uniform spin chain behavior [33]. Accordingly, experimental data were satisfactorily fitted to the Bonner–Fisher model, including a Curie-tail contribution at low temperatures with the following expression,  $\chi_{\text{mol}} = \chi_0 + x \cdot \chi_{\text{Curie}} + (1-x)\chi_{\text{BF}}$ , with  $\chi_0 = 1.6 \times 10^{-3} \text{ cm}^3 \text{ mol}^{-1}$ ,  $x = 2.2\%$   $S = 1/2$  magnetic defaults and  $|J|/k = 34.9(2)$  K, that is  $J = -24.5 \text{ cm}^{-1}$ . The origin of the spin chain behavior can be tentatively assigned to those uniform chains running along the *b*-direction as shown in Fig. 6. Indeed, a stronger antiferromagnetic interaction within the dyads identified above would introduce a spin gap in the system and a singlet ground state, not experimentally observed here.

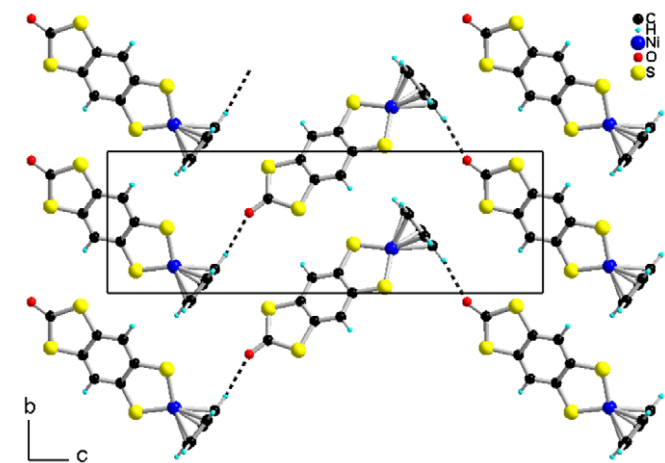


Fig. 4. A view of one layer in [CpNi(bdtodt)] showing the C–H···O=C hydrogen bond pattern.

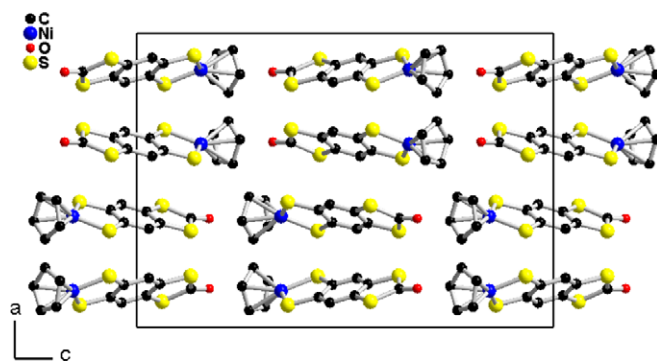


Fig. 5. A projection view of the unit cell of [CpNi(bdtodt)] along *b*.

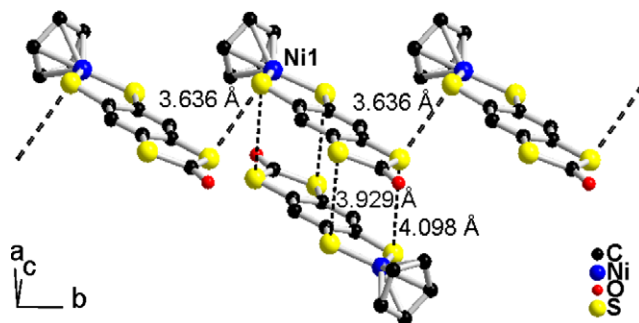


Fig. 6. A view of a complex with its nearest neighbors, forming an inversion centered dyad and chains of molecules running along *b*. Dotted lines indicate the shortest S··S intermolecular contacts.

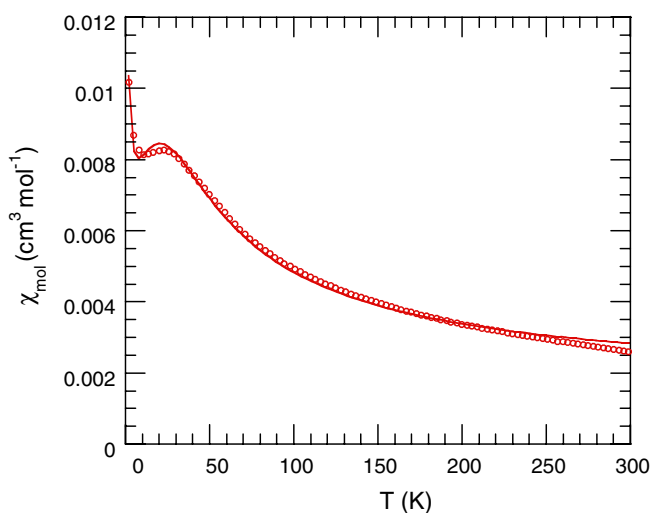


Fig. 7. Temperature dependence of the magnetic susceptibility of [CpNi(bdtodt)]. The solid line is a fit to the Bonner–Fisher model including a Curie tail (see text).

### 3. Conclusion

We have reported here the preparation, X-ray crystal structures, redox potentials and electronic absorption spectra of [CpCo(bdtodt)] and [CpNi(bdtodt)]. Both complexes are isostructural, as often observed in these series, demonstrating that the added electron in the  $17e^-$

[CpNi(dithiolene)] complexes does not modify substantially the molecular packing in the solid state. Comparison with other Co and Ni complexes shows some general trends with the low energy absorption band of the cobalt complexes observed around 550–680 nm moved toward lower energy in the analogous nickel complexes (700–1000 nm). TD-DFT calculations are in progress to assign those transitions and understand these trends. The paramagnetic nature of the [CpNi(bdtodt)] complex is revealed by its magnetic susceptibility and its temperature dependence is characteristic of the presence of uniform spin chains. The isostructural character of both compounds and this uniform spin chain behavior would allow for the preparation of such Heisenberg  $S = 1/2$  spin chains with variable doping of diamagnetic Co species, an interesting aspect in condensed matter physics.

## 4. Experimental

### 4.1. General remarks

All reactions were carried out under an argon atmosphere by means of standard Schlenk techniques. All solvents for chemical reactions were dried and distilled by Na-benzophenone for toluene and THF before use. Benzo[1,2-d;4,5-d']bis[1,3]dithiole-2,6-dione [34] and [CpCo(CO)I<sub>2</sub>] [35] were synthesized by literature methods. [Cp<sub>2</sub>Ni] was obtained from STREM Chemicals. Silica gel (Silica gel 60) was obtained from MERCK, Ltd. TOF-mass spectrum was recorded on a Bruker Daltonics MALDI-TOF BIFLEX III mass spectrometer. UV–Vis and NIR spectra were recorded on a Hitachi Model UV-2500PC. Elemental analyses were performed by the “Service d’Analyse du CNRS” at Gif/Yvette, France.

### 4.2. Preparation of [CpCo(bdtodt)]

Benzo[1,2-d;4,5-d']bis[1,3]dithiole-2,6-dione (104 mg, 0.4 mmol) was treated with potassium *tert*-butoxide (180 mg, 1.6 mmol) in THF solution (50 mL) at room temperature. The colorless solution changed to cloudy yellow after 30 min. When [CpCo(CO)I<sub>2</sub>] (325 mg, 0.8 mmol) was added, the yellow solution was rapidly changed to dark blue. The reaction mixture was further stirred at room temperature for 30 min. After the solvent was removed under reduced pressure, the residue was separated by column chromatography on silica gel with dichloromethane/petroleum ether 2:1(v/v) as eluant. The product was further purified by recrystallization in dichloromethane/petrol ether at –30 °C. [CpCo(bdtodt)] was obtained as dark blue crystals in 55% yield. Mass (EI<sup>+</sup>, 1.3 kV)  $m/z$  354 (M<sup>+</sup>). HR-MS (EI<sup>+</sup>) Calcd. For C<sub>12</sub>H<sub>7</sub>CoOS<sub>4</sub>: 353.87117. Found: 353.8696. <sup>1</sup>H NMR (CDCl<sub>3</sub>, 200 MHz, vs. TMS)  $\delta$  = 5.57 (s, 5 H, Cp), 8.22 (s, 2H, benzene). UV–Vis–NIR (CH<sub>2</sub>Cl<sub>2</sub>)  $\lambda_{\max}/\text{nm}$  ( $\epsilon$ ) 293 (77,000), 595 (24,000). Anal. Calc. for C<sub>12</sub>H<sub>7</sub>CoOS<sub>4</sub>: C, 40.67; H, 1.99; S, 36.19. Found: C, 40.26; H, 2.00.

### 4.3. Preparation of [CpNi(bdtodt)]

A toluene solution (30 mL) of [Cp<sub>2</sub>Ni] (567 mg, 3.0 mmol) and benzo[1,2-d;4,5-d']bis[1,3]dithiole-2,6-dione (78 mg, 0.3 mmol) were reacted under reflux for 24 h. After the solvent was removed under reduced pressure, the residue was dissolved in dichloromethane. The mixture solution was transferred into a column chromatography on silica gel, and a red fraction was collected by dichloromethane/*n*-hexane eluent (2:1(v/v)). The product was further purified by recrystallization (dichloromethane/*n*-hexane). [CpNi(bdtodt)] was obtained as dark red crystals in 26% yield. TOF-Mass (MALDI, 19 kV)  $m/z$  353 (M<sup>+</sup>). UV–Vis–NIR (CH<sub>2</sub>Cl<sub>2</sub>)  $\lambda_{\max}/\text{nm}$  ( $\epsilon$ ) 326 (37,000), 741 (6000). Anal. Calc. for C<sub>12</sub>H<sub>7</sub>NiOS<sub>4</sub>: C, 40.70; H, 1.99; S, 36.22. Found: C, 40.42; H, 2.05; S, 36.45.

### 4.4. X-ray diffraction studies

The single crystals of [CpM(bdtodt)] (M = Co and Ni) complexes were obtained by recrystallization from the dichloromethane solutions and then vapor diffusion of *n*-hexane into those solutions. A crystal was mounted on the top of a thin glass fiber. Data were collected on a Stoe Imaging Plate Diffraction System (IPDS) for [CpNi(bdtodt)] and on a Kappa CCD Diffractometer for [CpCo(bdtodt)], with graphite-monochromated Mo K $\alpha$  radiation ( $\lambda = 0.71073$  Å) at room temperature. Structures were solved by direct methods (SHELXS-97) and refined (SHELXL-97) [36] by full-matrix least-squares methods, as implemented in the WINGX software package [37]. Absorption corrections were applied. Hydrogen atoms were introduced at calculated positions (riding model), included in structure factor calculations, and these were not refined. Crystallographic data of complexes are summarized in Table 4.

### 4.5. CV measurements

All electrochemical measurements were performed under an argon atmosphere. Solvents for electrochemical measurements were dried by 4 Å molecular sieve before use. A platinum wire served as a counter electrode, and the reference electrode is SCE (saturated calomel electrode) was corrected for junction potentials by being referenced internally to the ferrocene/ferrocenium (Fc/Fc<sup>+</sup>) couple. A stationary platinum disk (1.0 mm in diameter) was used as a working electrode. CV measurements were performed with an Autolab PGSTAT 20 potentiostat from Eco Chemie B.V., equipped with General Purpose Electrochemical System GPES software (version 4.5 for Windows). Solution resistance was compensated by positive feedback. 1 mmol dm<sup>–3</sup> dichloromethane solutions of dithiolene complexes containing 0.1 mol dm<sup>–3</sup> tetrabutylammonium hexafluorophosphate (NBu<sub>4</sub>PF<sub>6</sub>) at 25 °C were used for measurements.

Table 4  
Crystallographic data of [CpM(bdtodt)] (M = Co and Ni) complexes

Compound	[CpCo(bdtodt)]	[CpNi(bdtodt)]
Formula	C <sub>12</sub> H <sub>7</sub> CoOS <sub>4</sub>	C <sub>12</sub> H <sub>7</sub> NiOS <sub>4</sub>
FW (g mol <sup>-1</sup> )	354.35	354.13
Crystal color	Dark blue	Dark red
Crystal shape	Plate	Plate
Crystal size (mm)	0.12 × 0.09 × 0.03	0.75 × 0.60 × 0.01
Crystal system	Orthorhombic	Orthorhombic
Space group	<i>Pbca</i> (No. 61)	<i>Pbca</i> (No. 61)
<i>a</i> (Å)	15.605(3)	15.6976(12)
<i>b</i> (Å)	7.2085(14)	7.2380(5)
<i>c</i> (Å)	22.488(5)	22.4487(19)
<i>V</i> (Å <sup>3</sup> )	2529.7(9)	2550.6(3)
<i>T</i> (K)	293(2)	293(2)
<i>Z</i>	8	8
<i>D</i> <sub>calc</sub> (g cm <sup>-3</sup> )	1.861	1.763
<i>μ</i> (mm <sup>-1</sup> )	1.996	1.844
Total reflections	5413	13726
Absorption correction	Multi-scan	Multi-scan
Unique reflections ( <i>R</i> <sub>int</sub> )	2907 (0.0278)	2466 (0.0772)
Unique reflections	2039 ( <i>I</i> > 2σ( <i>I</i> ))	1532 ( <i>I</i> > 2σ( <i>I</i> ))
<i>R</i> <sub>1</sub> , <i>wR</i> <sub>2</sub>	0.0437, 0.1056 ( <i>I</i> > 2σ( <i>I</i> ))	0.0518, 0.1326 ( <i>I</i> > 2σ( <i>I</i> ))
<i>R</i> <sub>1</sub> , <i>wR</i> <sub>2</sub> (all data)	0.0702, 0.1201	0.0867, 0.1544
Goodness-of-fit	1.085	0.878

$$R_1 = \sum ||F_o| - |F_c|| / \sum |F_o|; wR_2 = [\sum w(F_o^2 - F_c^2)^2 / \sum wF_o^4]^{1/2}.$$

#### 4.6. Magnetic susceptibility measurements

Magnetic susceptibility measurements were performed on a Quantum Design MPMS-2 SQUID magnetometer operating on the range of 2–300 K at 5000 G with a polycrystalline sample of [CpNi(bdtodt)] (2.5 mg). Molar susceptibilities were corrected for Pascal diamagnetism. Fit to the uniform chain model are based on the following expression (Eq. (1)) of the spin Hamiltonian, and the total susceptibility of the [CpNi(bdtodt)] complex was fitted with Eq. (2) [33,38] where *x* is the fraction of *S* = 1/2 magnetic defaults (Curie tail):

$$H = -J \sum_1^{n-1} S_{A_i} S_{A_{i+1}} \quad (1)$$

$$\chi_{\text{mol}} = \chi_0 + x \cdot \frac{Ng^2\beta^2}{2kT} + (1-x) \frac{Ng^2\beta^2}{kT} \frac{0.25 + 0.074975x + 0.075235x^2}{1 + 0.9931x + 0.172135x^2 + 0.757825x^3} \quad (2)$$

with  $x = |J|/kT$ .

#### Acknowledgements

We thank Professor Masatsugu Kajitani (Sophia University) for some UV–Vis–NIR measurements and Thierry Roisnel (Rennes) for the X-ray data collections. We also thank for the Ministère de la Recherche (France) and the ANR (France) (CHIRASYM Project) for a post-doctoral grant (to M.N.).

#### Appendix A. Supplementary material

CCDC 624495 and 624496 contain the supplementary crystallographic data for ([CpCo(bdtodt)]) and ([CpNi(bdtodt)]). These data can be obtained free of charge via <http://www.ccdc.cam.ac.uk/conts/retrieving.html>, or from the Cambridge Crystallographic Data Centre, 12 Union Road, Cambridge CB2 1EZ, UK; fax: (+44) 1223-336-033; or e-mail: [deposit@ccdc.cam.ac.uk](mailto:deposit@ccdc.cam.ac.uk). Supplementary data associated with this article can be found, in the online version, at [doi:10.1016/j.jorgchem.2007.02.030](https://doi.org/10.1016/j.jorgchem.2007.02.030).

#### References

- [1] (a) C.L. Beswick, J.M. Schulman, E.I. Stiefel, *Prog. Inorg. Chem.* 52 (2003) 55; (b) K. Wang, *Prog. Inorg. Chem.* 52 (2003) 267.
- [2] G.N. Schrauzer, *Acc. Chem. Res.* 2 (1969) 72, and references therein.
- [3] (a) R.B. King, *J. Organomet. Chem.* 623 (2001) 95; (b) P. Falaras, C.-A. Mitsopoulou, D. Argyropoulos, E. Lyris, N. Psaroudakis, E. Vrachnou, D. Katakis, *Inorg. Chem.* 34 (1995) 4536; (c) R. Eisenberg, E.I. Stiefel, R.C. Rosenberg, H.B. Gray, *J. Am. Chem. Chem.* 88 (1966) 2874; (d) G.N. Schrauzer, V.P. Mayweg, *J. Am. Chem. Chem.* 88 (1966) 3235.
- [4] M. Roger, T. Arliguie, P. Thuery, M. Fourmigué, M. Ephritikhine, *Inorg. Chem.* 44 (2005) 584.
- [5] M. Roger, T. Arliguie, P. Thuery, M. Fourmigué, M. Ephritikhine, *Inorg. Chem.* 44 (2005) 594.
- [6] (a) D. Sellmann, J. Sutter, *Prog. Inorg. Chem.* 52 (2003) 585; (b) S.D. Cummings, R. Eisenberg, *Prog. Inorg. Chem.* 52 (2003) 315.
- [7] M. Fourmigué, *Coord. Chem. Rev.* 178 (1998) 823, and references therein.
- [8] M. Fourmigué, *Acc. Chem. Res.* 37 (2004) 179.
- [9] (a) R. Clérac, M. Fourmigué, C. Coulon, *J. Solid State Chem.* 159 (2001) 413;



- (b) R. Clérac, M. Fourmigué, J. Gaultier, Y. Barrans, P.A. Albouy, C. Coulon, *Eur. Phys. J. B* 9 (1999) 445;
- (c) B. Domercq, M. Fourmigué, *Eur. J. Inorg. Chem.* 6 (2001) 1625;
- (d) M. Fourmigué, B. Domercq, I.V. Jourdain, P. Molinie, F. Guyon, J. Amaudrut, *Chem. Eur. J.* 4 (1998) 1714;
- (e) M. Fourmigué, C. Lenoir, C. Coulon, F. Guyon, J. Amaudrut, *Inorg. Chem.* 34 (1995) 4979;
- (f) J.K. Hsu, C.J. Bonangelino, S.P. Kaiwar, C.M. Boggs, J.C. Fettinger, R.S. Pilato, *Inorg. Chem.* 35 (1996) 4743.
- [10] (a) M. Fourmigué, N. Avarvari, *Dalton Trans.* (2005) 1365;
- (b) M. Nomura, R. Okuyama, C. Fujita-Takayama, M. Kajitani, *Organometallics* 24 (2005) 5110;
- (c) M. Nomura, T. Cauchy, M. Geoffroy, P. Adkine, M. Fourmigué, *Inorg. Chem.* 45 (2006) 8194;
- (d) M. Nomura, M. Geoffroy, P. Adkine, M. Fourmigué, *Eur. J. Inorg. Chem.* (2006) 5012.
- [11] C. Takayama, M. Kajitani, T. Sugiyama, A. Sugimori, *J. Organomet. Chem.* 563 (1998) 161.
- [12] (a) E.J. Miller, T.B. Brill, A.L. Rheingold, W.C. Fultz, *J. Am. Chem. Soc.* 105 (1983) 7580;
- (b) M. Fourmigué, V. Perrocheau, *Acta Crystallogr. C* 53 (1997) 1213.
- [13] T.B. Rauchfuss, *Prog. Inorg. Chem.* 52 (2003) 1.
- [14] A. Sugimori, T. Akiyama, M. Kajitani, T. Sugiyama, *Bull. Chem. Soc. Jpn.* 72 (1999) 879.
- [15] R.B. King, *J. Am. Chem. Soc.* 85 (1963) 1587.
- [16] C. Faulmann, F. Delpech, I. Malfant, P. Cassoux, *J. Chem. Soc., Dalton Trans.* (1996) 2261.
- [17] (a) W. Kusters, P. De Mayo, *J. Am. Chem. Soc.* 96 (1974) 3502;
- (b) W. Schroth, H. Bahn, R. Zschernitz, *Z. Chem.* 13 (1973) 424;
- (c) R. Schulz, A. Schweig, K. Hartke, J. Koester, *J. Am. Chem. Soc.* 105 (1983) 4519.
- [18] (a) D.-Y. Noh, M. Mizuno, J.-H. Choy, *Inorg. Chim. Acta* 216 (1994) 147;
- (b) M. Mizuno, *Synth. Met.* 56 (1993) 2154.
- [19] N.C. Schiødt, P. Sommer-Larsen, T. Bjørnholm, M.F. Nielsen, J. Larsen, K. Bechgaard, *Inorg. Chem.* 34 (1995) 3688.
- [20] E. Fanghaenel, J. Bierwisch, A. Ullrich, A. Herrmann, *Chem. Ber.* 128 (1995) 1047.
- [21] K. Heinze, G. Huttner, L. Zsolnai, *Z. Naturforsch., B: Chem. Sci.* 54 (1999) 1147.
- [22] H. Köpf, H. Balz, *J. Organomet. Chem.* 387 (1990) 77.
- [23] D. Sellmann, M. Geck, F. Knoch, G. Ritter, J. Dengler, *J. Am. Chem. Soc.* 113 (1991) 3819.
- [24] K. Shimizu, H. Ikehara, M. Kajitani, H. Ushijima, T. Akiyama, A. Sugimori, G.P. Satô, *J. Electroanal. Chem.* 396 (1995) 465.
- [25] F. Guyon, D. Lucas, I.V. Jourdain, M. Fourmigué, Y. Mugnier, H. Cattey, *Organometallics* 20 (2001) 2421.
- [26] F. Guyon, I.V. Jourdain, M. Knorr, D. Lucas, T. Monzon, Y. Mugnier, N. Avarvari, M. Fourmigué, *Eur. J. Inorg. Chem.* (2002) 2026.
- [27] M. Nomura, M. Fujii, K. Fukuda, T. Sugiyama, Y. Yokoyama, M. Kajitani, *J. Organomet. Chem.* 690 (2005) 1627.
- [28] (a) J. Moraczewski, W.E. Geiger, *J. Am. Chem. Soc.* 103 (1981) 4779;
- (b) M.M. Bernardo, P.V. Robant, R.R. Schroeder, D.B. Rorabacher, *J. Am. Chem. Soc.* 111 (1989) 1224;
- (c) A.M. Bond, R. Colton, T.F. Mann, *Organometallics* 7 (1988) 2224;
- (d) C. Tsintavis, H.-I. Li, J.Q. Chambers, *J. Phys. Chem.* 95 (1991) 289;
- (e) T.C. Richards, W.E. Geiger, *J. Am. Chem. Soc.* 116 (1994) 2028;
- (f) N.G. Connelly, W.E. Geiger, M.C. Lagunas, B. Metz, A.L. Rieger, P.H. Rieger, M.J. Shaw, *J. Am. Chem. Soc.* 117 (1995) 12202.
- [29] C. Takayama, E. Suzuki, M. Kajitani, T. Sugiyama, A. Sugimori, *Organometallics* 17 (1998) 4341.
- [30] T. Akiyama, Y. Watanabe, A. Miyasaka, T. Komai, H. Ushijima, M. Kajitani, K. Shimizu, A. Sugimori, *Bull. Chem. Soc. Jpn.* 65 (1992) 1047.
- [31] G.R. Desiraju, T. Steiner, *The Weak Hydrogen Bond*, Oxford University Press, Oxford, 1991.
- [32] M. Fourmigué, P. Batail, *Chem. Rev.* 104 (2004) 5379.
- [33] O. Kahn, in: *Molecular Magnetism*, VCH, 1993, pp. 251–284 (Chapter 11).
- [34] J. Larsen, K. Bechgaard, *J. Org. Chem.* 52 (1987) 3285.
- [35] R.B. King, *Inorg. Chem.* 5 (1966) 82.
- [36] G.M. Sheldrick, *SHELX97 – Programs for Crystal Structure Analysis* (Release 97-2), 1998.
- [37] L.J. Farrugia, *J. Appl. Cryst.* 32 (1999) 837.
- [38] W. E. Estes, D.P. Gavel, W.E. Hatfield, D. Hodgson, *Inorg. Chem.* 17 (1978) 1415.